Gold nanoparticles superlattices assembly for electrochemical biosensor detection of MicroRNA-21

Liang Tian, Kun Qian, Jinxu Qi, Qinyao Liu, Chen Yao, Wei Song, Yihong Wang

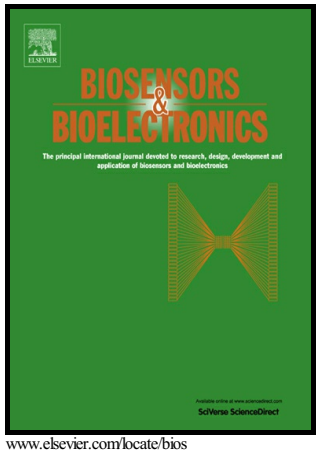

www.elsevier.com/locate/bios

PII: S0956-5663(17)30570-5
DOI: http://dx.doi.org/10.1016/j.bios.2017.08.035
Reference: BIOS9945

To appear in: *Biosensors and Bioelectronic*

Received date: 29 April 2017
Revised date: 13 August 2017
Accepted date: 13 August 2017

Cite this article as: Liang Tian, Kun Qian, Jinxu Qi, Qinyao Liu, Chen Yao, Wei Song and Yihong Wang, Gold nanoparticles superlattices assembly for electrochemical biosensor detection of MicroRNA-21, *Biosensors and Bioelectronic,* http://dx.doi.org/10.1016/j.bios.2017.08.035

Gold nanoparticles superlattices assembly for electrochemical biosensor detection of MicroRNA-21

Liang Tian, Kun Qian, Jinxu Qi, Qinyao Liu, Chen Yao, Wei Song, Yihong Wang*

School of Chemistry and Chemical Engineering, Southeast University, Nanjing, 211189, P.R.China.

Abstract

Gold nanoparticles (AuNPs) superlattice and small molecule dyes such as toluidine blue have remarkable effect on signal amplification. In this report, a label-free and simple electrochemical microRNA biosensor is developed by employing toluidine blue (TB) as a redox indicator and AuNPs superlattice as a support material. Conductive polymer, polypyrrole coated AuNPs was self-assembled to form a superlattice which exhibited the most close-packed type thereby producing the maximum current. The successful immobilization of the single strand RNA (ss-RNA) probe and hybridization with the target microRNA sequence were confirmed by electrochemical cyclic voltammetry (CV) methods as well as differential pulse voltammetry (DPV) technique, which was used to determine the oxidation peak current of TB under optimal condition. TB with efficient signal amplification was applied in microRNA biosensor for the first time. By employing this strategy, microRNA can be detected in a range from 100 aM to 1 nM with a relatively low detection limit of 78 aM. Alongside the outstanding sensitivity and selectivity, this nanobiosensor had great reproducibility and showed a remarkable response in the real sample analysis with serum samples. In conclusion, the proposed electrochemical nanobiosensor could be clinically useful in the early detection of the breast cancer by direct detection of the serum microRNA-21 in real clinical samples without sample preparation, RNA extraction and/or amplification.

Keywords：Electrochemical biosensor, Breast cancer, AuNPs superlattice, Toluidine blue, MicroRNA-21

1. Introduction

Cancer afflicts all communities in a worldwide range and is known as one of the leading causes of death, with breast cancer being one of the most common invasive type in women globally and its early detection is the key to the high potential, easy, inexpensive and most effective therapy. Early detection of cancer biomarkers could timely diagnose specific diseases as well as provide treatment for such before it develops into its later period, thereby increasing the survival rate of patients. In vitro diagnostic (IVD) test is a crucial component of clinical care that performs a diagnostic test on biological samples that have been taken from a living body, such as blood, urine,

and tissue (Zhou et al., 2015). Such tests are usually conducted to confirm the presence and determine the level of some diseases in an individual.

MicroRNAs are short single-stranded ribonucleic acid (RNA) molecules of about 19-23 nucleotides in length, which can play important regulatory roles in animals and plants by targeting microRNAs for cleavage or translational repression (Dong et al., 2013). As an important circulating microRNA, microRNA-21 is a robust oncogenic microRNA whose overexpression plays a significant role in the process of carcinogenesis and can be used as a biomarker for diagnosis, staging, progression and prognosis of the breast cancer (Shen et al., 2015). In addition, they are perfectly stable in serum, hence their sampling would be easy and non-invasive. Furthermore, it can also be used as a perfect biomarker for early detection of breast cancer. Due to their intrinsic properties of short length, low abundance and sequence homology among family members, it is difficult to realize sensitive and selective detection with economical use of time and cost. The traditional methods for microRNA analysis are northern blotting (Lagos-Quintana et al., 2001), microarray analysis (Lim et al., 2005) and real-time quantitative polymerase chain reaction (qRT-PCR), but they are very time-consuming, sample-consuming, and semi-quantitative with low sensitivity and throughput.

In recent years, electrochemical biosensor technology has received greater attention by the virtue of its unique detection, analysis methods and the potential applications in clinical diagnostic. Electrochemical nanobiosensors are emerging field of biosensors which combines the advantages of electrochemical biosensing with nanotechnology, thereby generating a new class of low cost, robust, reliable, easy-to-use and ultrasensitive diagnostics (Turner, 2013; Xia et al., 2013; Hou et al., 2015). Nanomaterials hold unique physicochemical properties that offer desirable and unmatched characteristics for chemical and biological detection such as significant surface area to volume ratio, strong signal intensities, and finely tunable surface chemistries (Miao et al., 2015). To date, many studies based on various nanomaterials, such as carbon nanotubes, silica nanowires, quantum dots (QDs), magnetic nanoparticles, AuNPs, just to mention a few, have been targeted at creating high-sensitivity in vitro diagnostic (IVD) systems for biomarkers (Li et al., 2016). Due to their excellent conductivity, high surface area, good biocompatibility and catalytic properties, AuNPs are ideal platforms for electrochemical biosensor detection. While the electrodes of most biosensors are constructed by simply dropping nanoparticles onto the electrodes' surface, random pack of the nanoparticles may block many active sites, thereby reduce the number of biomolecules that bind to nanoparticles (Ye et al., 2015). Thus, there is an immediate need for ordered array of nanoparticles and more active sites in specific area of electrode to provide highly sensitive biomarker detection.

Nowadays nanoparticles superlattices have shown a variety of applications in biosensing, catalysis, photonic crystals, nanoelectronics and energy conversion and storage (Paik et al., 2015). Spontaneous organization of inorganic nanoparticles (NPs) into superlattices is of great interest due to the new and advanced collective properties of the assemblies, exhibiting a wide range of stoichiometries and lattice symmetries (Li et al., 2016). Ordered arrays of NPs demonstrate a tunable structure and property. The patterned nanoparticles are closely packed, hence eliminate the block of many active sites and provide efficient active sites on specific area of the electrode surface. In particular, interparticle interactions in NPs superlattices can lead to new, collective properties, which are significantly different from isolated NPs. More importantly, the NPs superlattices are capped with pristine or polymer, hence exhibit physical properties which are

strongly dependent on inorganic core size of the NPs, the packing ratio of NPs and their dimensionality (Li et al., 2015). At a specific size ratio and concentration ratio of nanoparticles, the assembled superlattices become most densely packed which could improve conductivity and also accelerate electronic transmission. The most densely packed superlattices were suitable for use as an electrode surface support material due to their excellent electrical conductivity and large surface area, thereby providing more active sites in combination with capture probes.

Toluidine blue (TB) is an aromatic heterocyclic dye which interacts with nucleic acid sequence and can be employed as hybridization indicator in the design of electrochemical nucleic acid biosensor (Rafiee-Pour et al., 2016). The possible mechanism of TB and microRNA interaction has been established via electrostatic interaction with negatively charged backbone phosphate groups. Then toluidine blue interacted with small groove of single stranded DNA or RNA through hydrophobic effect, and intercalated into large groove of the duplex DNA or RNA through π-π stack, forming hydrogen bonds with DNA or RNA bases (Tavallaie et al., 2014; Peng et al., 2015; Nguyen et al., 2016). The behavior of TB linked to single- and double-stranded oligonucleotides has been studied using both spectroscopy and electrochemistry methods (Azimzadeh et al., 2016). In this work TB was employed to interact with microRNA in microRNA biosensor for the first time. Depending on the binding mode of TB-microRNA complex, either decrease or increase in the voltammetric response after hybridization is reported for quantification of nucleic acid sequences. The main advantage of TB linking mode is that microRNA can be determined without any laborious labeling and operation complexity. Furthermore, with the advantages of molecular structure, TB has better flatness and could form hydrogen bonds easier with RNA skeleton, hence promotes more intercalation into RNA skeleton than previously reported methylene blue (Bai et al., 2014).

Herein, AuNPs superlattices was modified onto the electrode to enlarge the specific surface area and electrical conductivity for the first time. A novel convenient and label-free platform for sensitive detection of microRNA was presented, which is based on TB as a hybridization indicator. Due to the excellent electron transport capability and tunable structures capacity of AuNPs superlattices, the remarkable improvement of the immobilizing amount of probe molecules on the electrode surface and a great enhancement of the electrical signal of the substrate were achieved, after which a label-free electrochemical biosensor for detecting microRNA-21 is prepared.

2. Experimental

2.1. Chemicals and materials

Synthetic capture probes ss-RNA and microRNA sequences used in this work were purchased from Sangon Biotech Co., Ltd. (Shanghai, China). All chemicals were purchased from Sigma Aldrich and used without further purification. The buffer solutions used in this work are as follows. Buffer for ss-RNA immobilization was 10 mM K_2HPO_4-citric acid containing 1.0 M NaCl (pH 5.4). Hybridization buffer was prepared with 1.0 SSC (Saline-Sodium Citrate) solution containing 15 mM tri-sodium citrate and 150 mM NaCl, while washing buffer solution was 0.1 SSC. A pH 7.4 phosphate-buffer solution (PBS, 20 mM phosphate buffer + 0.15 M NaCl) was used as the supporting electrolyte for differential pulse voltammetry (DPV) quantification. All solutions were treated with diethyl pyrocarbonate (DEPC) and all sample tubes, microtips and glassware were

autoclaved to minimize the effect of RNases on the stability of microRNAs. The oligonucleotide sequences are listed in Table S1. Artificial human serum samples used for the addition and recovery experiments of microRNA-21 were purchased from Sigma Aldrich (St. Louis, MO), and the human serum samples of breast cancer patients and healthy individuals were supplied by the affiliated hospital of Qingdao University. qRT-PCR data were supplied by KeyGEN-BioTECH (Nanjing, China).

2.2. Electrochemical apparatus and measurements

Electrochemical experiments were carried out with a CHI660E electrochemical workstation (Shanghai Chenhua Instruments, China). A conventional three-electrode system, consisting of a 3.0-mm diameter glassy carbon electrode (GCE), a saturated calomel electrode (SCE) as reference electrode and a platinum wire counter electrode were used in all electrochemical measurements. The electrochemical techniques are cyclic voltammetry (CV), AC impedance (EIS) and differential pulse voltammetry (DPV). Transmission electron microscopy (TEM) images were obtained from a Hitachi H-800 microscope (Japan), while UV-vis absorption spectrum was analyzed by Hitachi UH4150 UV-vis-NIR Spectrophotometer.

2.3. Gold nanoparticles synthesis and characterization

AuNPs were prepared by reducing $HAuCl_4$ with trisodium citrate according to previous reports (Hill et al., 2006; Liu et al., 2006). Briefly, 5 mL of 38.8 mM trisodium citrate was added rapidly into a stirred boiling aqueous solution containing 50 mL of 1 mM $HAuCl_4$ while stirring. The solution turned from clear to black, purple and deep red in sequence within 2 min. The solution was kept boiling with continuous stirring for 15 min, after which it was naturally cooled down to room temperature. The final colloidal solution was stored at 4 ℃ for further use. The concentration of AuNPs was calculated to be 13 nM using Beer-Lambert Law.

2.4. Synthesis of oligomer polypyrrole (ppy)

PPy were prepared according to previous reports (Wen et al., 2013; Mondal et al., 2015). The detail of the procedure is given as Supplementary information.

2.5. Gold nanoparticles ligand exchange

Polypyrrole-based ligands were attached to the AuNPs surface by a simple ligand-exchange reaction. In a typical process, the as-synthesized AuNPs were dissolved in 5 mL of tetrahydrofuran (THF) at a NP concentration of 5 mg mL^{-1}. Another 5 mL THF solution of polypyrrole was prepared separately with a polymer concentration of 40 mg mL^{-1}. The polypyrrole solution was then added dropwise under sonication to the NPs solution and the resulting mixture was stirred for 24 h at room temperature to promote surface saturation with polymeric ligands. The polymer-modified NPs were then isolated by ethanol precipitation and centrifugation at 7,000 rpm for 3 min. The supernatant was removed and the NPs were redispersed in THF. The above solvent-nonsolvent cleaning procedure was repeated 4-6 times to remove excess unbound

polymers and the NPs were finally dispersed in toluene to a concentration of about 3 mg mL^{-1}.

2.6. Self-assemble of NPs superlattices and characterization

In the self-assemble process, 20 nm and 5 nm gold nanoparticles in molar ratio of C_{20}:C_5 =1:12 were dissolved in toluene containing capping ligand (e.g. oleic acid). Then about 40 μL of the above dispersions with a particle concentration of 1 mg/mL were placed in glass vials. The glass vial was sealed with a matched cap with a pore diameter of 0.5 mm as an outlet and tilted by 60-70°. Then GCE was immersed into the solution and was tilted at a certain angle. With the evaporation of the liquid, the surface of the GCE could form a layer of gold nanoparticle superlattice film (Smith et al., 2009; Kong et al., 2011). The self-assembly temperature was typically set at 45 ℃. After 5 h, the gold nanoparticles superlattices (AuNS) film was transferred onto a carbon-coated Cu TEM grid (300-mesh) or GCE for TEM and electrochemical characterization.

2.7. Preparation of the nanobiosensor

Prior to use, the bare GCE was thoroughly polished with a 1.0 μm and 0.05 μm alumina-water slurry on a smooth polishing cloth until a mirror-like surface was obtained. Successively, it was sonicated for 5 min in distilled deionized water to remove the alumina residual particles, and rinsed thoroughly with distilled water and dried under a nitrogen flow. The NS film was transferred on the cleaned GCE and allowed to dry at room temperature. Subsequently, the capture probe adsorption was accomplished by immersing AuNS modified GCE (AuNS/GCE) into 200 μL immobilization buffer (pH 5.4) containing 1.0 μM ss-RNA (as capture probe) at room temperature for 120 min. After the adsorption, the modified electrode (ss-RNA/AuNS/GCE) was gently rinsed with PBS to remove unbound ss-RNA probe. Then, the ss-RNA immobilized electrodes was incubated in 1.0 SSC containing the target microRNA-21 for 1.0 h to achieve hybridization (microRNA/ss-RNA/AuNS/GCE). The non-hybridized adsorbed microRNA could be removed from the biosensor surface when exposed to 0.1 SSC. The microRNA/ss-RNA/AuNS/GCE was immersed into TB solution (4.0 μM TB-0.2 M NaCl-0.10 M PBS pH 7.4) for 5 min. The modified electrodes were thereafter rinsed carefully with PBS to remove any excess of TB in order to ensure that the electrochemical signal obtained only accounts for TB bound to the sequences. Finally, the TB oxidation current was measured by DPV in PBS (pH 7.4). The whole detection process would take 3.5 h including every electrode modification steps and electrochemical detection steps. The electrochemical signal of TB was compared before and after hybridization and the significant increase in peak current was attributed to the target microRNA concentration. The analysis principle of the label-free electrochemical microRNA biosensor is depicted in Scheme 1.

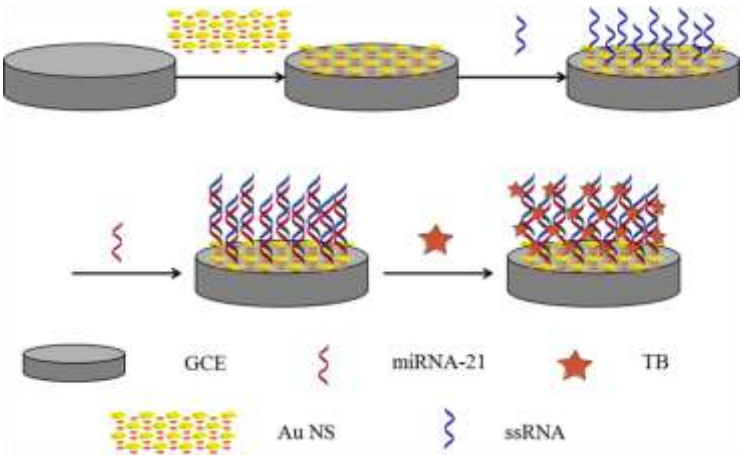

Scheme 1. Schematic representation of the microRNA biosensor and detection principle.

3. Results and discussion

3.1. Characterization of AuNPs superlattice

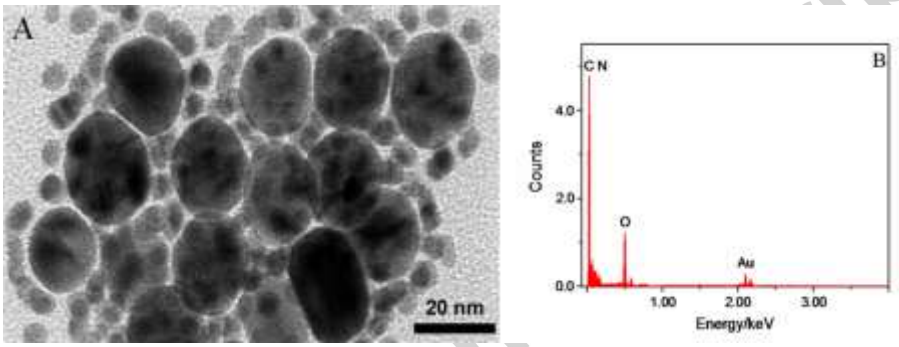

Fig. 1. Morphological and structure characterization of AuNPs superlattice: (a) TEM images of $CaCu_5$-type superlattice self-assembled from 20 nm and 5 nm AuNPs. (b) EDS analysis of AuNS.

Polypyrrole has π electrons with better electrical conductivity than Alkyl ligands, and the length of the ppy ligand is adjustable. Furthermore, the atom N on polypyrrole has many action sites with AuNPs, and could induce and drive AuNPs for superlattice assembly. The use of ppy ligand provides quantitative and precise control over nearest-neighbour interparticle distances. This is difficult, if not impossible, with the short alkyl-chain-based ligands that have been used in previous studies (Ng et al., 2012; Wang et al., 2016; Gu et al., 2017). To achieve the most densely packed superlattices, several size ratios and molar ratios of nanoparticles were used. Under a specific size ratio, when the nanoparticles molar ratio is reduced from ~15:1 to ~7:1 as used for $NaZn_{13}$, bcc-AB_6-type BNLSs were obtained. Further decrease in nanoparticles molar ratio resulted in the formation of phase-pure lower stoichiometry, including from $AuCu_3$, AlB_2 and NaCl to $MgZn_2$. The specification and quality of the synthesized AuNPs (PPy modified) were shown by UV-vis absorption spectrum (Fig. S1). According to literatures, in the formation of a specific $CaCu_5$-type superlattice with the size ratio of nanoparticles increases from 0 to 0.5, the size ratio of nanoparticles nearly 0.25 could obtain the maximum packing density (Ye et al., 2015). Thus we use 20 nm and 5 nm gold nanoparticles at size ratio of 0.25 to self-assemble to form close packed $CaCu_5$-type superlattice. A TEM image of the 2D AuNPs

superlattice was shown in Fig. 1A which exhibited a $CaCu_5$-type dispersion, while the thickness of the polypyrrole shell was approximately 1 nm. Moreover, the EDS analysis (Fig. 1B) shows the composition of the AuNPs superlattice. Compared with random pack of the nanoparticles, the AuNPs superlattice has a higher surface area, while the actual surface of the electrode was greatly increased to amplify the signals as well as increase the electron transfer. In addition, we also prepared most densely packed of NaCl-type superlattice in the size ratio of 0.4 and molar ratio of 4:1 as shown in Fig. S2. To confirm the excellent conductivity of AuNPs superlattice, cyclic voltammetry was employed to determine bare AuNPs and different types of AuNPs superlattices as shown in Fig. S3. By comparing these two superlattices, from figure S3 it could be obtained that the conductivity of $CaCu_5$-type and NaCl-type was comparable. From figure 3 and figure S4, the detection limit of $CaCu_5$-type modified biosensor was better. Thus, we chose the $CaCu_5$-type AuNS as electrode surface material of the biosensor.

3.2. Principle of the electrochemical biosensor

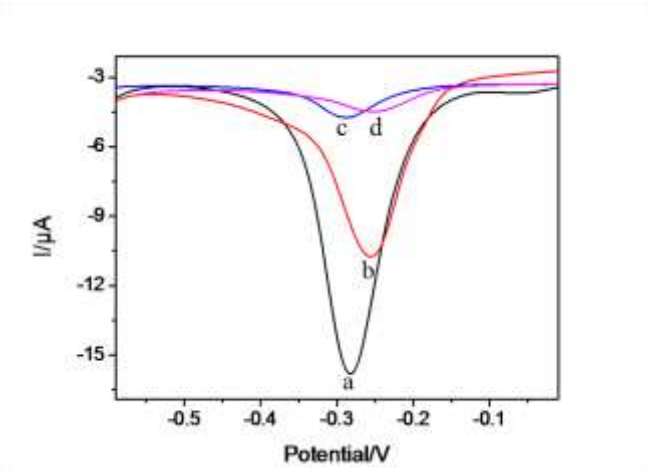

Fig. 2. DPV curves of different modified electrodes obtained in 0.01 M PBS: 1 nM microRNA modified SS-RNA probe/AuNS/GCE after incubated in 4 μM TB (a) or MB (b). SS-RNA probe/AuNS/GCE after incubated in 4 μM TB (c) or MB (d).

In this study, ss-RNA was used as probe which could hybridize with full match complementary target microRNA-21 via hydrogen bonding. The RNA-RNA hybrid molecules have greater stability as compared with DNA-RNA hybrid molecules (Melton et al., 1984; Cova et al., 1988; Kilic et al., 2013; Cardoso et al., 2016). TB was used as an electrochemical signal amplification indicator to investigate the quantity of the target microRNA sequence hybridized with the microRNA-21 probe. The toluidine blue has a π-π conjugated electron and has a better coexistence with the π-π electrons of the RNA bases. The planar heterocyclic dye TB is probable to stabilize its binding to single and double strand nucleic acid sequence through electrostatic, hydrogen bonding and favorable stacking interactions with its adjacent base pairs DNA. TB was oxidized to oxidation state with a quasi-reversible two electrons and one proton reaction at physiological pH. To further prove the effective signal amplification of the TB modified microRNA complex, different modified electrodes were investigated by DPV experiments. As shown in Fig. 2, there was an obvious redox peak of TB on the sandwiched microRNA complex modified GCE (curve a)

compared to the MB modified microRNA complex (curve b) in the presence of 1 nM of microRNA-21. The electrochemical detection of microRNA-21 was performed based on observing the current signal change of TB oxidation peak. TB has good conductivity and has higher affinity with double-stranded RNA than MB. Compared to MB molecule, TB molecule has better flatness and could easily form hydrogen bonds with RNA skeleton, thus enhances its intercalation to RNA skeleton than MB (Paul et al., 2013).

3.3. Characterization of biosensor fabrication

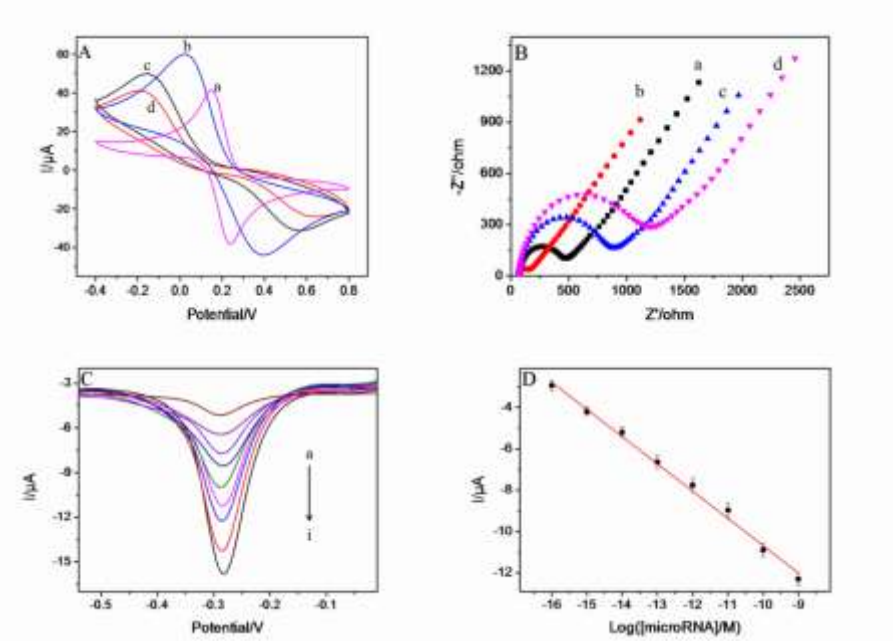

Fig. 3. Cyclic voltammograms (A) and EIS (B) of bare GCE (a), AuNS/GCE (b), SS-RNA probe/AuNS/GCE (c), and microRNA/SS-RNA probe/AuNS/GCE (d) in 5.0 mmol L^{-1} $Fe(CN)_6^{4-/3-}$ containing 0.1 mol L^{-1} KCl at 100 mV s^{-1}. (C) DPV responses to SS-RNA probe/AuNS/GCE fabricated biosensor after capturing different concentrations of microRNA-21 from (a) to (i): 0 M, 100 aM, 1 fM, 10 fM, 100 fM, 1 pM, 10 pM, 100 pM and 1 nM. (D) Calibration curve of peak current vs. logarithmic microRNA-21 concentration. Error bars=RSD (n=5).

The biosensor was characterized by electrochemical CV measurements, which provide more prolific information about the change of interface property of the microRNA modified electrode, since the decrease of redox peak is equal to the increase of the interfacial electrons transfer resistance. Fig. 3A shows the CV obtained in 0.5 mM $Fe(CN)_6^{4-/3-}$ solution containing 0.1 M KCl at different electrodes. AuNS modified GCE electrode exhibited a higher current redox peak of $Fe(CN)_6^{4-/3-}$ (curve b) with an enhanced electron transfer than bare GCE (curve a). After thiolated captured probe ss-RNA was self-assembled onto the electrode surface, the current redox peak of $Fe(CN)_6^{4-/3-}$ decreased significantly (curve c), because the oligonucleotides were non-conductive. When the GCE immersed in 1 nM target microRNA, the current voltammogram redox peak of $Fe(CN)_6^{4-/3-}$ further decreased (curve d) due to the steric hindrance of electron transfer after target microRNA-21 was hybridized with captured probe ss-RNA.

The detailed change in electron-transfer resistance (Ret) can be further detected by EIS. Fig. 3B shows the impedance spectra in the form of Nyquist plots of the interfaces recorded after each

modification step. Due to the good electronic transfer ability, the AuNS modified GCE (curve b) displayed an almost straight line in the Nyquist plot, exhibiting a lower Ret than the bare GCE (curve a). It was clear that the diameter of the semicircles successively increased with the sequential assembly of ss-RNA probe (curve c) and microRNA (curve d), indicating an enhancement in the Ret step by step. These results were well consistent with the phenomena in CVs, confirming the successful preparation of the biosensor.

3.4. Optimization of experimental parameters

To achieve optimal sensing performance, a key issue of nucleic acid hybridization biosensor is the hybridization time. The influence of the hybridization time was assessed for optimum analytical performance. The ss-RNA/AuNS/GCE was incubated with 1 nM microRNA-21 solution for 20, 40, 60, 80 and 120 min, with the recorded cyclic voltammograms being presented in Fig. S5. As shown in Fig. S5, after 60 min, the current signal approached a platform, hence 60 min was selected as the suitable incubating time between target microRNA-21 and probe ss-RNA. These results suggested the hybridization reaction was completed after 60 min, hence this value was adopted in the following work.

3.5. Performance of the biosensor

DPV has been found to be a sensitive electrochemical technique and is widely applied to analytical purposes. In this work, DPV revealed variations of the electrochemical response of TB after hybridization of ss-RNA capture probe with microRNA target (Fig. 3C). The peak current was attributed to the oxidation of TB on microRNA/ss-RNA/AuNS/GCE. The peak currents of the biosensor were linearly proportional to the logarithm of target microRNA-21 concentration. This oxidation peak current measured for different microRNA-21 concentration is presented as calibration curve in Fig. 3D. At least five replicates were performed for each microRNA-21 concentration to attain a calibration curve. The average oxidation peak current has a good linear relationship versus the logarithmic of microRNA-21 concentration in a range from 100 aM to 1 nM with the regression equation of I=-1.31915 logC-23.87564 (I is the peak current and C is the microRNA concentration, R^2=0.99417). The detection limit was estimated to be 78 aM at a signal to noise ratio of 3 (where was the standard deviation of the blank solution, n=5), which was comparable to those reported by most of microRNA-based assays and other electrochemical biosensing strategy for microRNA detection (Table 1).

Table 1 Comparison of different biosensors for determination of microRNA.

Target microRNA	Method of signal amplification	Electrode/Electrochemical methods	Linear range	Detection limit	References
microRNA-21	Hairpin capture probe/target recycling/MB	AuE/DPV	0.5 pM-2000 pM	56 fM	Zhou et al., 2017
microRNA-21	AuNPs/SA-ALP/redox cycling	AuE/Amp	10 fM-5 pM	3 fM	Liu et al., 2014

microRNA-21	MCH/Ir(Ⅲ)complex	AuE/CV	5 fM-1 pM	1.6 fM	Miao et al., 2016
microRNA-377	Capture probe/MCH/ST-AP	AuE/DPV	1 fM-2 nM	0.68 fM	Hu et al., 2017
microRNA-155	GO/GNR/OB	GCE/DPV	2 fM-8 pM	0.6 fM	Azimzadeh et al., 2016
microRNA-21	AuNPs/capture probe/redox cycling	AuE/DPV	1 fM-100 pM	0.36 fM	Li et al., 2016
microRNA-21	Au@CoFe2O4/Tb-Gra/rolling circle amplification	GCE/SWV	1fM-2nM	0.3 fM	Yu et al., 2017
microRNA-24	AuNPs/Pd@HRP	GCE/DPV	3 fM-1 nM	0.2 fM	Wu et al., 2016
microRNA-21	MoS2/AuNPs/SA-ALP	GCE/DPV	0.1 fM-0.1 pM	0.086 fM	Shuai et al., 2017
microRNA-21	AuNS/capture probe/TB	GCE/DPV	100 aM-1 nM	78 aM	This work

3.6. Selectivity and reproducibility of the biosensor

Another important feature of a good biosensor is high selectivity. To examine the selectivity of our proposed biosensor, a comparison study on mismatch targets and perfect complementary target was performed. Fig. 4A shows the voltammograms for the different kinds of targets including the perfect complementary target microRNA-21, single-base mismatch microRNA-21 and non-complementary target microRNA at a concentration of 1 nM respectively. As expected, the oxidation peak current of complementary target microRNA-21 is higher than other mismatched sequence and non-complementary sequence, which demonstrated that our proposed biosensor showed high selectivity for the perfect complementary target microRNA-21. Furthermore, the reproducibility of the biosensor was also investigated. Electrode surface prepared on the same and different electrodes were used to detect microRNA-21 at the same concentration. Standard deviation of five dependent measurements was less than 5 % for the same electrode, and less than 8 % for six different electrodes, as shown in Fig. 4. Thus, the developed biosensor shows good reproducibility.

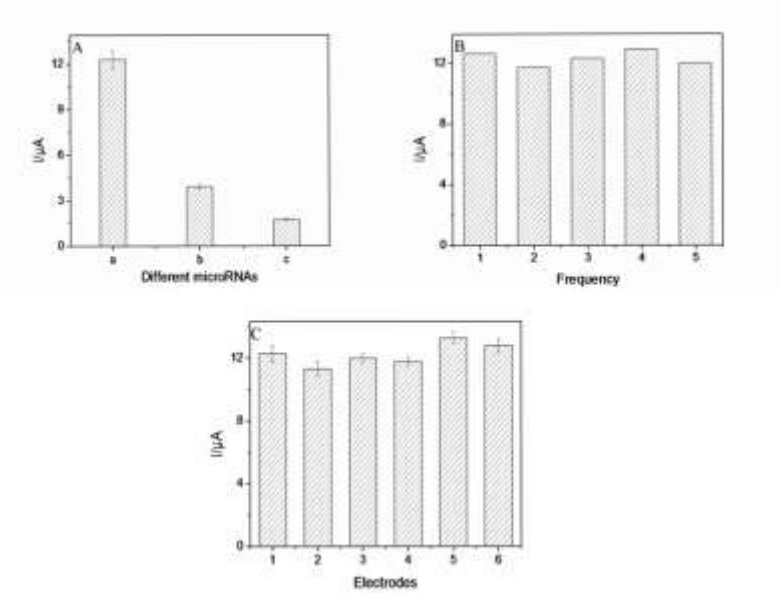

Fig. 4. (A) DPV responses of the proposed biosensor in specificity for complementary target microRNA-21 (a), single-base mismatch microRNA (b) and non-complementary microRNA (c). The concentrations were 1nM respectively. The electrochemical DPV response of same fabricated biosensors for five times (B), and independently fabricated 6 biosensors (C). The concentrations were 1 nM respectively. Error bars=RSD (n=5).

3.7. Analytical application of the proposed biosensor

To evaluate the applicability of the proposed biosensor, the standard addition method was employed. A series of real samples were prepared by adding different concentrations of microRNA-21 into human serum. All experiments were performed in compliance with the relevant laws and institutional guidelines, with full approved by the Institution's Committee. The analytical results for microRNA-21 were shown in Table S2. It could be seen that the recovery was between 91.3 % and 105.8 % and relative standard deviation was below 4.13 %, which indicated that the prepared electrochemical microRNA biosensor had promising analytical applications in real biological samples. Meantime, the concentrations of microRNA-21 in human serums were detected by using our assay and qRT-PCR method. As shown in Fig. S6, the detection results obtained by using our assay were consistent with those of the qRT-PCR method, which correspond to previous reports (Liu et al., 2012; Zhang et al., 2016). Employing this rapid and convenient method will assist medical researchers to clarify microRNA-21 target network and find out the way of using microRNA-21 as biomarker for cancer prediction and treatment.

4. Conclusions

We have successfully developed an ultrasensitive electrochemical biosensor for rapid, sensitive, and quantitative detection of microRNA-21 by using AuNPs superlattice as a support material with TB as signal amplification molecules. PPy-coated AuNPs self-assembly into orderly arrangement superlattice would achieve the most close-packed type to obtain the maximum current and thereby improve the efficiency of electron transfer. TB with efficient signal amplification was applied in microRNA biosensor for the first time, which exhibited significantly

enhanced redox activities than MB. Furthermore, the AuNPs superlattice and TB played an excellent role in signal amplification of the biosensor. The detection limit of the proposed biosensor was increased by using TB as signal-amplifying nanoprobes. The proposed electrochemical biosensor can sensitively detect microRNA-21 in a range from 100 aM to 1 nM with a detection limit of 78 aM. It also exhibited good selectivity and acceptable reproducibility for microRNA-21 detection, which will have a promising potential for microRNA-21 detection in real serum samples. Finally, the proposed biosensor will not only be suitable for determining microRNA-21 as shown above but also for other interesting tumor markers.

Acknowledgements

This research was financially supported by the National Nature Science Foundations of China (No. 81571812) and A Project Funded by the Priority Academic Program Development of Jiangsu Higher Education Institutions (1107047002).

References

Azimzadeh, M., Rahaie, M., Nasirizadeh, N., Ashtari, K., Naderi-Manesh, H., 2016. Biosens. Bioelectron. 77, 99-106.

Bai, L.J., Chai, Y.Q., Pu, X.Y., Yuan, R., 2014. Nanoscale 6, 2902-2908.

Cardoso, A.R., Moreira, F.T.C., Fernandes, R., Sales, M.G.F., 2016. Biosens. Bioelectron. 80, 621-630.

Cova, L., Kopecka, H., Aymard, M., Girard, M., 1988. J. Med. Virol. 24, 11-18.

Dong, H.F., Lei, J.P., Ding, L., Wen, Y.Q., Ju, H.X., Zhang, X.J., 2013. Chem. Rev. 113, 6207-6233.

Hill, H.D., Mirkin, C.A., 2006. Nat. Protoc. 1, 324-336.

Hou, T., Li, W., Liu, X.J., Li, F., 2015. Anal. Chem. 87, 11368-11374.

Hu, R., Wang, G.L., Yuan, R., Xu, Y.J., Yu, T.X., Zhong, L., Zhou, Q., Ding, S.J., 2017. J. Electroanal. Chem. 789, 160-166.

Gu, X.W., Ye, X.C., Koshy, D.M, Vachhani, S., Hosemann, P., Alivisatos, A.P., 2017. P. Natl. Acad. Sci. USA. 114, 2836-2841.

Kilic, T., Topkaya, S.N., Ozsoz, M., 2013. Biosens. Bioelectron. 48, 165-171.

Kong, X., Zhao, J., Han, J., Zhang, D., Wei, M., Duan, X., 2011. Electrochim. Acta. 56, 1123-1129.

Lagos-Quintana, M., Rauhut, R., Lendeckel, W., Tuschl, T., 2001. Science 294, 853-858.

Li, B.C., Liu, F., Peng, Y.Y., Zhou, Y.L., Fan, W.X., Yin, H.S., Ai, S.Y., Zhang, X.S., 2016. Biosens. Bioelectron. 79, 307-312.

Lim, L.P., Lau, N.C., Garrett-Engele, P., Grimson, A., Schelter, J.M., Castle, J., Bartel, D.P., Linsley, P.S., Johnson, J.M., 2005. Nature 433, 769-773.

Li, P.H., Li, Y., Zhou, Z.-K., Tang, S.Y., Yu, X.-F., Xiao, S., Wu, Z.Z., Xiao, Q.L., Zhao, Y.T., Wang, H.Y., Chu, P.K., 2016. Adv. Mater. 28, 2511-2517.

Liu, J.W., Lu, Y., 2006. Nat. Protoc. 1, 246-252.

Liu, L., Xia, N., Liu, H.P., Kang, X.J., Liu, X.S., Xue, C., He, X.L., 2014. Biosens. Bioelectron. 53, 399-405.

Liu, Y.-Q., Zhang, M., Yin, B.-C., Ye, B.-C., 2012. Anal. chem. 84, 5165-5169.

Li, W., Hou, T., Wu, M., Li, F., 2016. Talanta 148, 116-121.

Li, W.K., Wang, K., Zhang, P., He, J., Xu, S.Y., Liao, Y.G., Zhu, J.T., Xie, X.L., Nie, Z.H., 2015. Small 12, 499-505.

Melton, D.A., Krieg, P.A., Rebagliati, M.R., Maniatis, T., Zinn, K., Green, M.R., 1984. Nucleic acids research 12, 7035-7056.

Miao, P., Wang, B.D., Yu, Z.Q., Zhao, J., Tang, Y.G., 2015. Biosens. Bioelectron. 63, 365-370.

Miao, X.M., Wang, W.H., Kang, T.S. Liu, J.B., Shiu, K.-K., Leung, C.-H., Ma, D.-L., 2016. Biosens. Bioelectron. 86, 454-458.

Mondal, S., Sangaranarayanan, M.V., 2015. Eur. Polym. J. 71, 596-611.

Ng, K.C., Udagedara, I.B., Rukhlenko, I.D., Chen, Y., Tang, Y., Premaratne, M., Cheng, W., 2012. Acs Nano 6, 925-934.

Nguyen, K.V., Holade, Y., Minteer, S.D., 2016. ACS Catal. 6, 2603-2607.

Paik, T., Diroll, B.T., Kagan, C.R., Murray, C.B., 2015. J. Am. Chem. Soc. 137, 6662-6669.

Paul, P., Kumar, G.S., 2013. J. Hazard. Mater. 263, 735-745.

Peng, H.-P., Hu, Y., Liu, P., Deng, Y.-N., Wang, P., Chen, W., Liu, A.-L., Chen, Y.-Z., Lin, X.-H., 2015. Sensor. Actuat. B-Chem. 207, 269-276.

Rafiee-Pour, H.-A., Behpour, M., Keshavarz, M., 2016. Biosens. Bioelectron. 77, 202-207.

Shen, W., Yeo, K.H., Gao, Z.Q., 2015. Analyst 140, 1932-1938.

Shuai, H.-L., Huang, K.-J., Chen, Y.-X., Fang, L.-X., Jia, M.-P., 2017. Biosens. Bioelectron. 89, 989-997.

Smith, D.K., Goodfellow, B., Smilgies, D.M., Korgel, B.A., 2009. J. Am. Chem. Soc. 131, 3281-3290.

Tavallaie, R., Darwish, N., Gebala, M., Hibbert, D.B., Gooding, J.J., 2014. ChemElectroChem 1, 165-171.

Turner, A. P. F., 2013. Chem. Soc. Rev. 42, 3184-3196.

Wang, K., Jin, S.-M., Xu, J.P., Liang, R.J., Shezad, K., Xue, Z.G., Xie, X.L., Lee, E., Zhu, J.T., 2016. Acs Nano 10, 4954-4960.

Wen, Q., Pan, X., Hu, Q.-X., Zhao, S.-J, Hou, Z.-F., Yu, Q.-Z., 2013. Synthetic. Met. 164, 27-31.

Wu, Y.M., Sheng, K., Liu, Y.Q., Yu, Q., Ye, B.X., 2016. Anal. Chim. Acta. 948, 1-8.

Xia, N., Deng, D.H., Zhang, L.P., Yuan, B.Q., Jing, M., Du, J.M., Liu, L., 2013. Biosens. Bioelectron. 43, 155-159.

Ye, X.C., Zhu, C.H., Ercius, P., Raja, S.N., He, B., Jones, M.R., Hauwiller, M. R., Liu, Y., Xu, T., Alivisatos, P., 2015. Nat. Commun. 6, 10052.

Yu, N., Wang, Z., Wang, C.C., Han, J., Bu, H.Y., 2017. Anal. Chim. Acta. 962, 24-31.

Zhang, J., Wu, D.-Z., Cai, S.-X., Chen, M., Xia, Y.-K., Wu, F., Chen, J.-H., 2016. Biosens. Bioelectron. 75, 452-457.

Zhou, L.L., Wang, J., Chen, Z.P., Li, J.L., Wang, T., Zhang, Z., Xie, G.M., 2017. Microchim. Acta. 184, 1305-1313.

Zhou, W., Gao, X., Liu, D.B., Chen X.Y., 2015. Chem. Rev. 115, 10575-10636.

Highlights

1. A novel electrochemical biosensor was developed for circulating microRNA-21 detection.
2. The nanoparticle superlattice was used to amplify the electrochemical signals.
3. The toluidine blue with higher affinity used as microRNA intercalative label.
4. A lower detection limit of 78 aM was obtained with good selectivity and repeatability.
5. The human plasma assay proved its potential for clinical breast cancer detection.

Graphical abstract